Supplementary Material

N-TiO_2 Photonic and Quantum Photocatalytic Efficiency Determined by Monte Carlo Simulation

Patricio F. F. Carnelli [1,2], Estefanía B. Bracco [1,†], Orlando M. Alfano [3] and Roberto J. Candal [1,*]

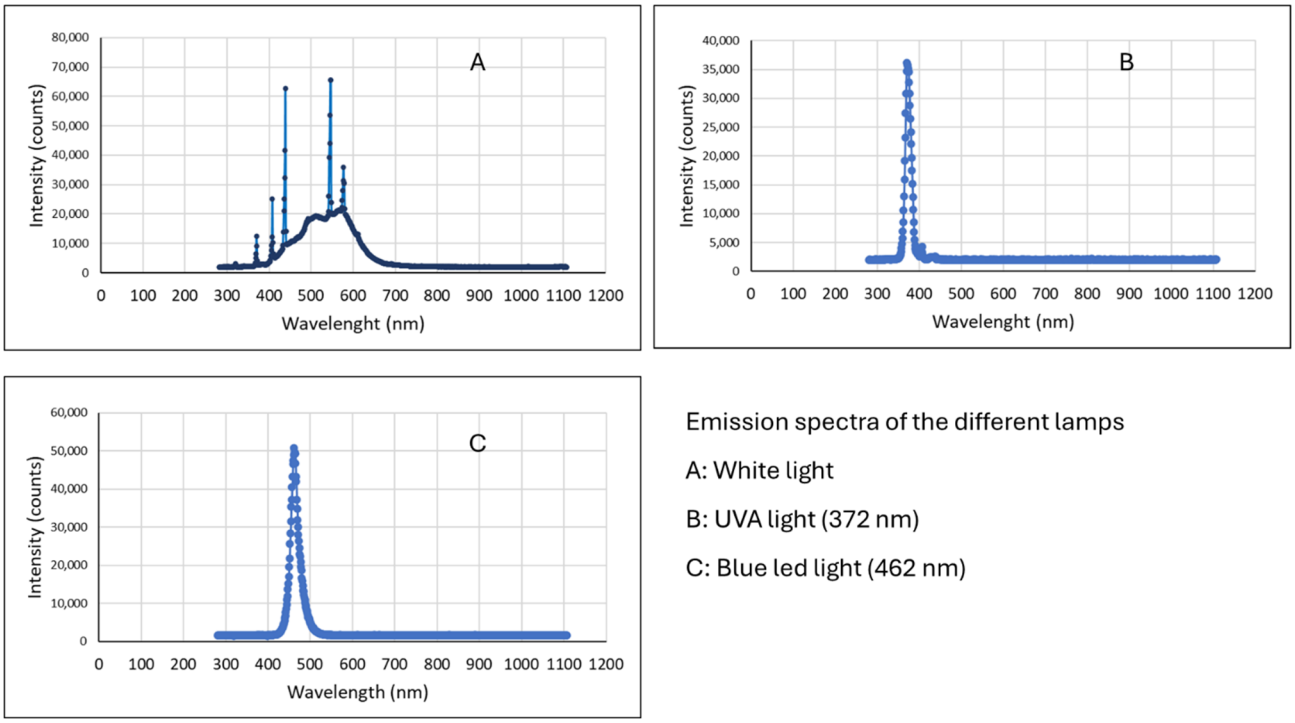

Figure S1. Emission spectra of the different lamps; Calculations and theory: Implementation of Monte Carlo simulations to calculate photon absorption efficiency.

Radiant flux or radiant energy per unit time (Einstein/s).
$\Phi e_{WL} = 0.49 \times 10^{-6}$
$\Phi e_{FWL} = 0.22 \times 10^{-6}$
$\Phi e_{UVA} = 0.76 \times 10^{-6}$
$\Phi e_{BL} = 1.01 \times 10^{-6}$

https://doi.org/10.70322/prp.2025.10019

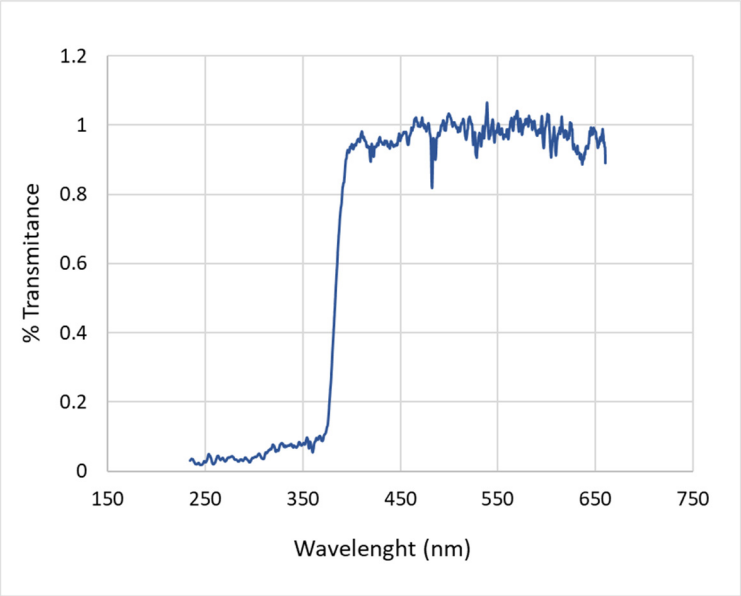

Figure S2. %Transmittance of cylindrical UV filter (commercial methacrylate). Cut Off ≈ 375 nm.

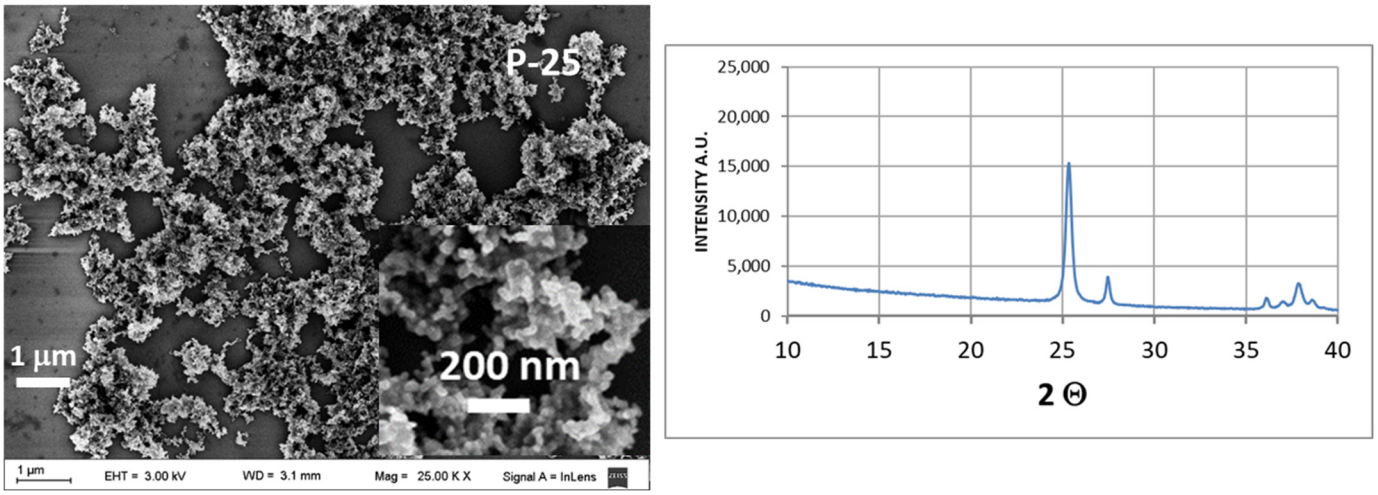

Figure S3. SEM image and DRX of TiO_2 P-25.

A quantitative phase analysis using Rietveld refinement was performed with the software MAUD (version 2.9995). The results indicated that the crystalline phase are Anatase (85%) and rutile (15%).

Implementation of Monte Carlo simulations to calculate photon absorption efficiency

In order to determine the photon trajectories, it is necessary to know their directions and lengths and the fate of the photons: absorption, scattering or loss. Absorption and scattering phenomena depend on the radiation wavelength. In this work we discretized the emission spectra of the radiation sources in 1 nm steps for the 300-550 nm wavelength range (as a reference, the 372 nm peak of the UVA source has a full width at half maximum of 20 nm). For the application of the Monte Carlo method, we implemented the following procedure:

i) Initial photon azimuthal angle ($_0$) and position (x_0, y_0, z_0): an initial azimuthal angle $_0$, between 0 and 2 is selected randomly from a uniform distribution (Eq. (S1)). The components of the initial position vector are then obtained by Eqs. (S1-S4), where D is the vessel diameter and L is the vessel height. The initial vertical position is also drawn from a uniform random distribution between $-L/2$ and $L/2$.

$$\varphi_0 = 2\pi R_1 \quad \text{(S1)}$$

$$x_0 = (D/2)\cos\varphi \quad \text{(S2)}$$

$$y_0 = (D/2)\sin\varphi \quad \text{(S3)}$$

$$z_0 = (L/2)(2R_2 - 1) \tag{S4}$$

where R_i (i=1, 2,…,7) are randomly generated numbers.

ii) Initial direction of photon trajectory ($\hat{x}_0, \hat{y}_0, \hat{z}_0$): since the initial direction of the photons is perpendicular to the lateral wall of the vessel, the values of the direction cosines $\hat{x}_0$ and $\hat{y}_0$ are determined by $_0$ and $\hat{z}_0$ should be null. Nevertheless, given the symmetrical setup of the lamps and the metallic coating of the case containing the reactor, the radiation that arrives to the internal side of the lateral wall can be considered as being diffuse. Therefore, there is a random variation included in the direction cosines according to Eqs. (S5-S8) where the vector ($\hat{x}', \hat{y}', \hat{z}'$) is properly normalized to obtain ($\hat{x}_0, \hat{y}_0, \hat{z}_0$).

$$\varphi' = (\pi/2)(2R_3 - 1) \tag{S5}$$

$$\hat{x}' = \cos(\pi + \varphi_0 - \varphi') \tag{S6}$$

$$\hat{y}' = \sin(\pi + \varphi_0 - \varphi') \tag{S7}$$

$$\hat{z}' = 2R_4 - 1 \tag{S8}$$

iii) Trajectory segment length (l) and new position: the distance that the photon can travel in the reaction medium without interacting (free path) is calculated by Eq. (S9) [Yokota et al., 1999].

$$l = -\frac{1}{\beta_\lambda}\ln(1 - R_5) \tag{S9}$$

where $\beta_\lambda = \sigma_\lambda + \kappa_\lambda$ is the extinction coefficient. Therefore, the new photon position $\vec{x}_{\text{new}}$ is determined by:

$$\vec{x}_{\text{new}} = \vec{x}_{\text{old}} + l(\hat{x}, \hat{y}, \hat{z})_{\text{old}} \tag{S10}$$

where the subscript "old" indicates the previous photon position and direction cosines. The previous direction cosines may be the initial ones or the ones obtained after a scattering event (using the phase function as explained below).

iv) Photon fate: if the photon is still inside the reaction medium after travelling a distance l, it interacts with a catalyst particle with two possible outcomes: absorption or scattering. The probability of occurrence of each event is related to the albedo ω_λ, defined as:

$$\omega_\lambda = {}^{\sigma_\lambda}/_{\beta_\lambda} \tag{S11}$$

The albedo varies between 0 and 1, where 1 means total scattering and 0 means total absorption. In this way, if

$$1 - \omega_\lambda \geq R_6 \tag{S12}$$

the photon is absorbed, and its trajectory ends. If not, the photon is scattered, and a new direction is determined by the phase function.

The phase function is specified by the scattering problem being modeled and may be complex enough to generate a great impact on the performance of the simulation. Hence, it is desirable to use a phase function that maintains the principal characteristics of the actual one and at the same time it is efficient to evaluate. Having this purpose in mind, the Henyey-Greenstein (HG) phase function was chosen. The HG phase function has one parameter only and can reproduce several other scattering probability functions. It is given by [Siegel and Howell, 2002]:

$$p_{HG,\lambda}(\cos\phi) = \frac{1 - {g_\lambda}^2}{2(1 + {g_\lambda}^2 - 2g_\lambda\cos\phi)^{3/2}} \tag{S13}$$

where g_λ is the asymmetry factor, which varies between -1 and 1 and depends on the wavelength. A value of 0 for the g_λ represents an isotropic phase function. If g_λ takes positive (negative) values, it means that the scattering is mainly produced in the forward (backward) direction.

From the HG phase function, the cosine of the scattering angle relative to the previous photon direction is [Moreira et al., 2010]:

$$\cos\phi = \frac{1}{2g_\lambda}\left[1 + {g_\lambda}^2 - \left(\frac{1 - {g_\lambda}^2}{1 + g_\lambda\,(2R_7 - 1)}\right)^2\right] \tag{S14}$$

Using the angle and an auxiliary random angle δ, the new direction cosines are obtained by trigonometric calculations. Assuming that scattering is azimuthally symmetric around the direction of incidence, the angle δ is uniformly distributed between 0 and 2π. The initial direction cosines are rotated to obtain the new direction cosines after scattering as follows:

$$\hat{x}_{\text{new}} = \frac{\sin\phi}{\alpha}(\hat{y}_{\text{old}}\,\sin\delta - \hat{x}_{\text{old}}\,\hat{z}_{\text{old}}\,\cos\delta) + \hat{x}_{\text{old}}\,\cos\phi \tag{S15}$$

$$\hat{y}_{\text{new}} = -\frac{\sin\phi}{\alpha}(\hat{x}_{\text{old}}\,\sin\delta + \hat{y}_{\text{old}}\,\hat{z}_{\text{old}}\,\cos\delta) + \hat{y}_{\text{old}}\,\cos\phi \tag{S16}$$

$$\hat{z}_{\text{new}} = \sin\phi\;\alpha\,\cos\delta + \hat{z}_{\text{old}}\,\cos\phi \tag{S17}$$

The term $\alpha = \sqrt{1 - \hat{z}_{\text{old}}^2}$ represents the transformation into a coordinate system where the z-axis is aligned with the initial direction. The terms involving the angles ϕ and δ implement the rotation.

Once the new direction is obtained, a new value of l is calculated, and the algorithm steps are repeated until the photon is absorbed or abandons the reaction medium. A flowchart of the described algorithm can be found in Figure S2.

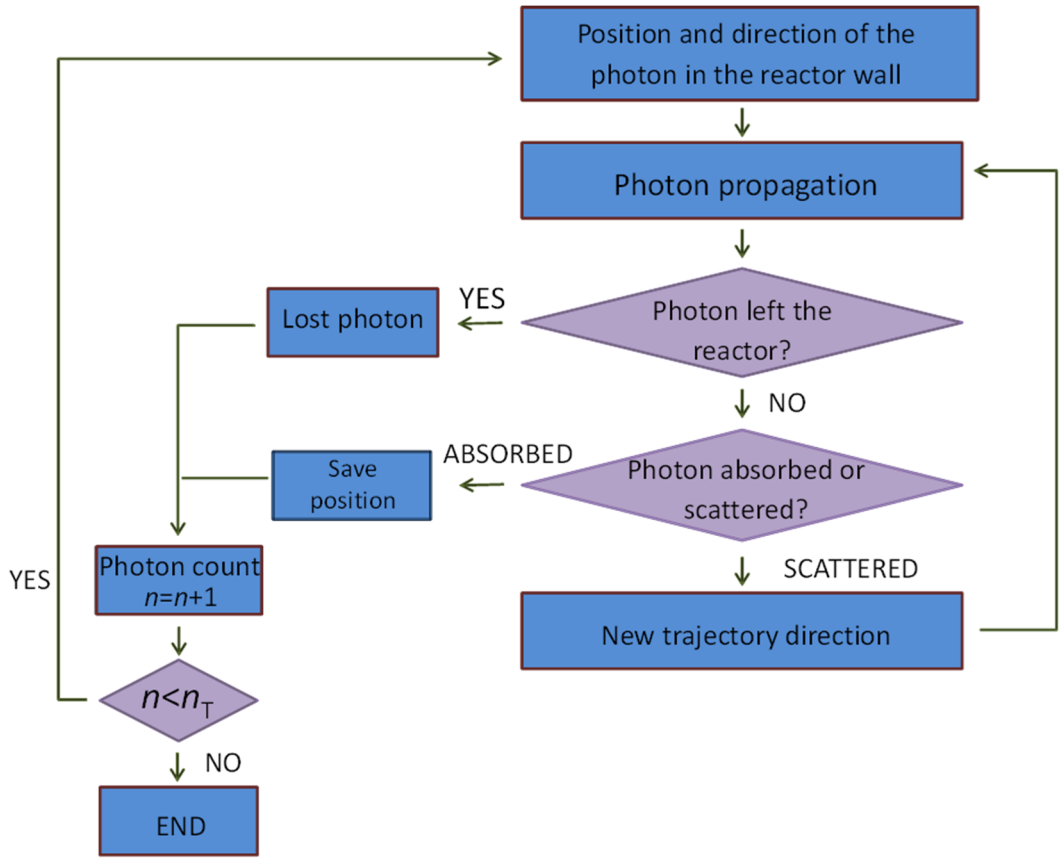

Figure S4. Flowchart of the Monte Carlo algorithm used for the simulation of the reactor, where n is the number of photons extinguished and n_T is the total number of photons at the beginning of the simulation.

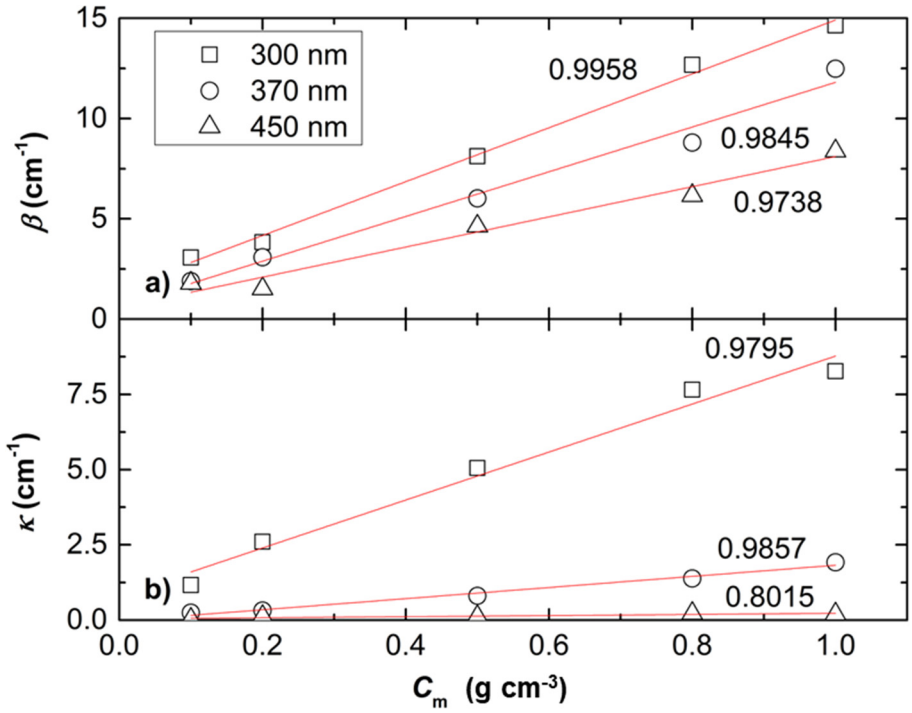

Figure S5. Coefficients of extinction (a) and absorption (b) as a function of concentration for three different wavelengths, for the N-TiO_2 photocatalyst. Also included are linear regressions for each dataset with their respective values for the coefficient of determination R^2

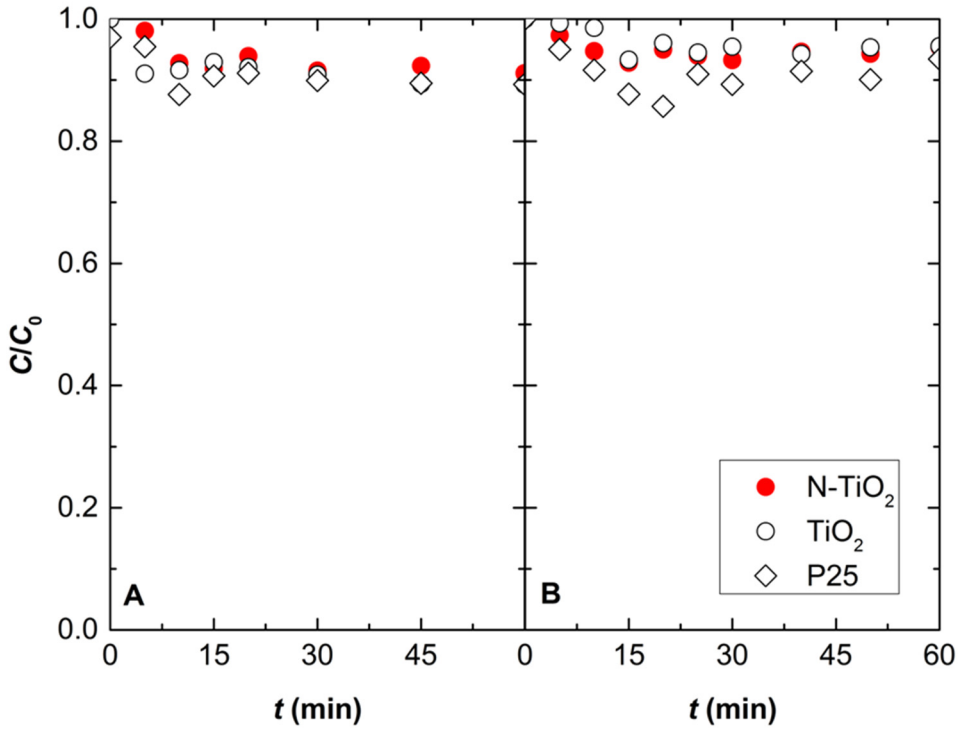

Figure S6. Time evolution of the concentration for the adsorption experiments (absence of irradiation) corresponding to formic acid (A) and salicylic acid (B).

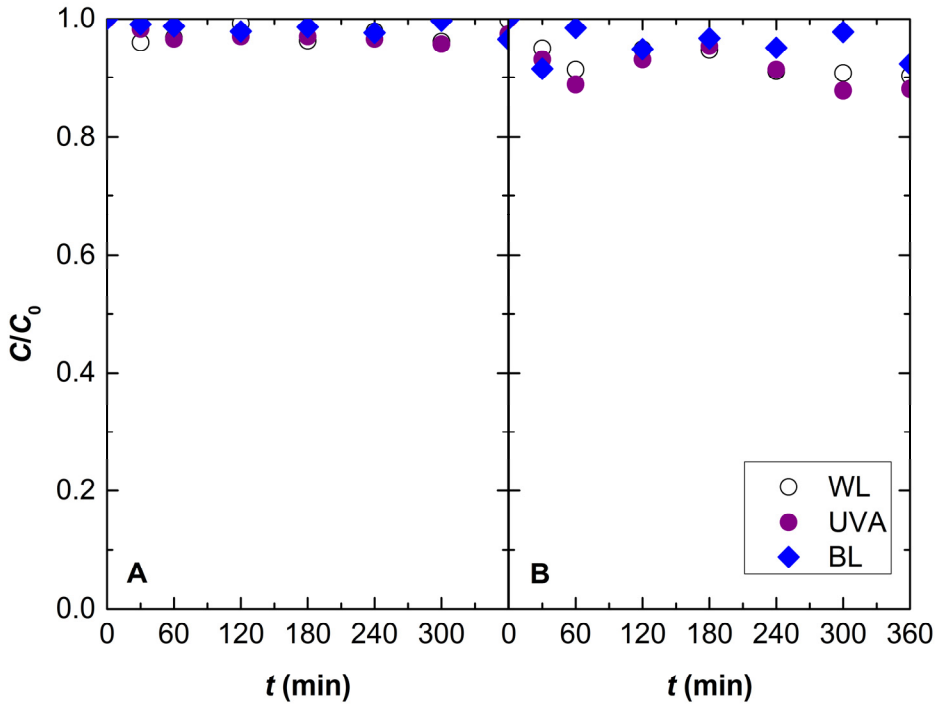

Figure S7. Effect of irradiation on aqueous solutions of: A) formic acid (2.5×10^{-4} M); B) Salicylic acid (1.0×10^{-4} M)

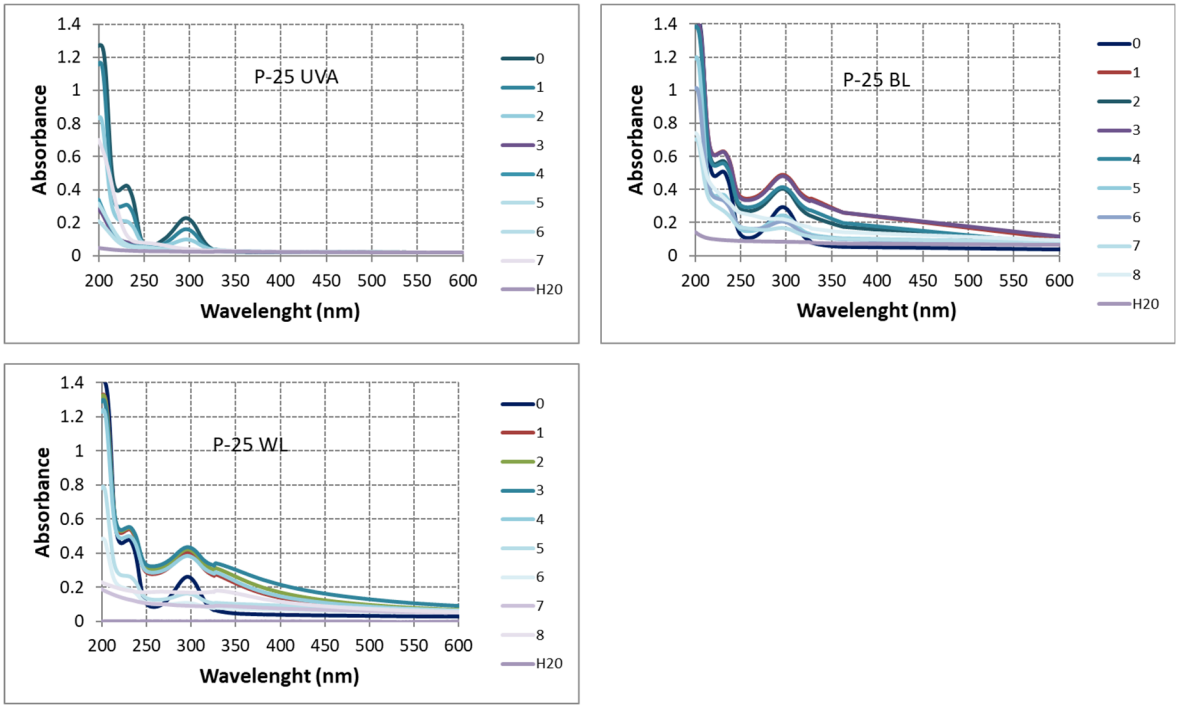

Figure S8. Absorption spectra of salicylic acid after different photocatalytic treatment times. Photocatalyst: P-25. Light source: UVA, white light (WL) and blue light (BL).

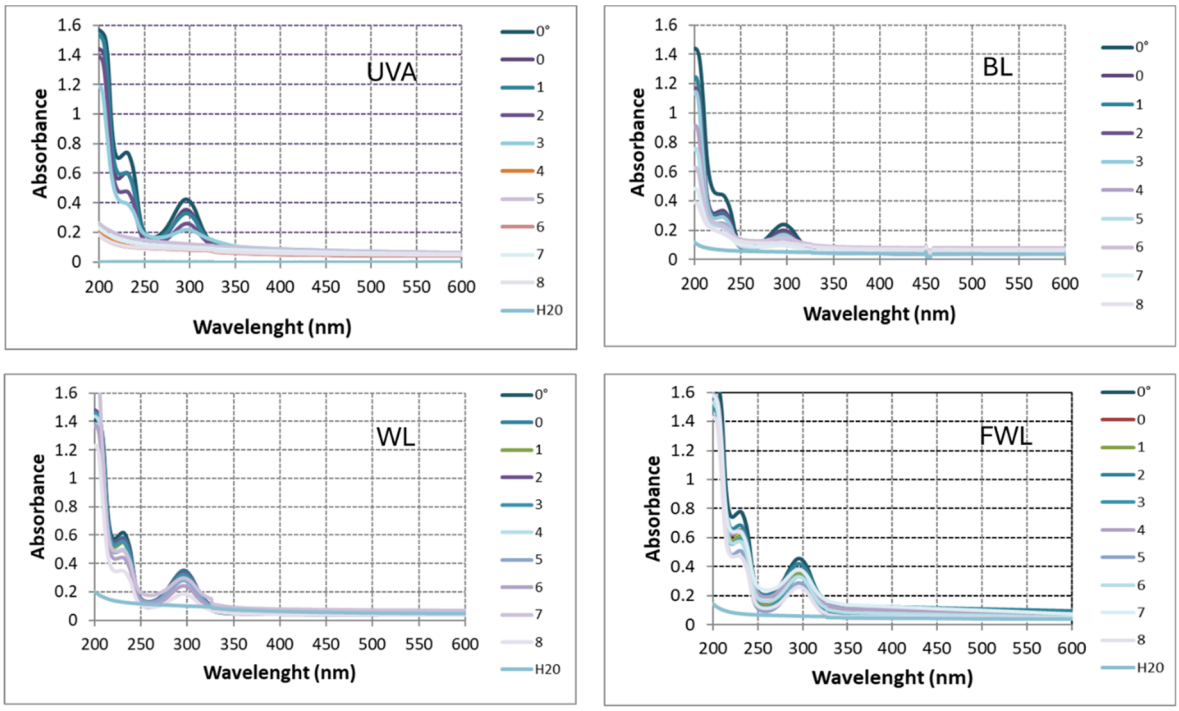

Figure S9. Absorption spectra of salicylic acid after different photocatalytic treatment times. Photocatalyst: N-TiO_2. Light source: UVA, white light (WL), filtered white light (FWL), and blue light (BL).

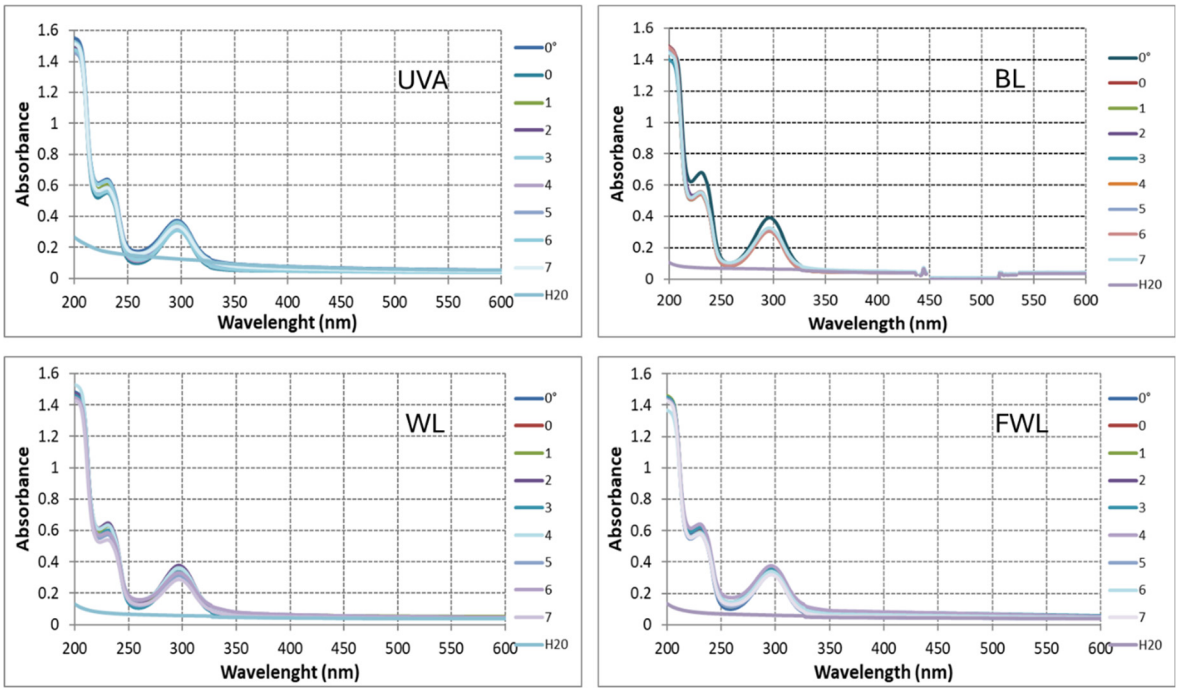

Figure S10. Absorption spectra of salicylic acid after different photocatalytic treatment times. Photocatalyst: TiO_2. Light source: UVA, white light (WL), filtered white light (FWL), and blue light (BL).

Table S1. Sum of squared residuals (SSR) of the fits of the concentration vs. time curves for the different photocatalysts. The considered models were the pseudo-order zero (Ord 0), pseudo-order 1 (Ord 1), and Langmuir-Hinshelwood (L-H) (for some example plots, see Fig. S7). The fitted values of the initial rate of reaction v_0 for the Ord 0 model are also included.

Pollutant	Light	Catalyst	SSR			v_0 (mol·cm^{-3}·s^{-1})
			Ord 0	Ord 1	L-H	
Formic Acid	White	N-TiO_2	0.480	4.330	10.88	1.83E-6
		P25	0.010	0.400	0.420	2.50E-6
	UV	N-TiO_2	0.100	3.280	1.690	9.83E-6
		TiO_2	0.030	0.120	0.110	7.00E-6
		P25	0.790	2.540	1.020	1.28E-5
Salicylic Acid	White	N-TiO_2	6.000	71.02	38.40	2.87E-5
		TiO_2	38.87	120.1	200.8	1.57E-4
		P25	121.0	146.5	434.9	6.28E-5
	UV	N-TiO_2	5.500	117.2	24.29	1.31E-4
		TiO_2	1.670	64.17	185.8	6.13E-5
		P25	12.49	281.4	716.9	2.37E-4
	Blue	N-TiO_2	4.100	7.300	8.080	1.85E-5
		P25	17.19	19.09	21.26	1.22E-5

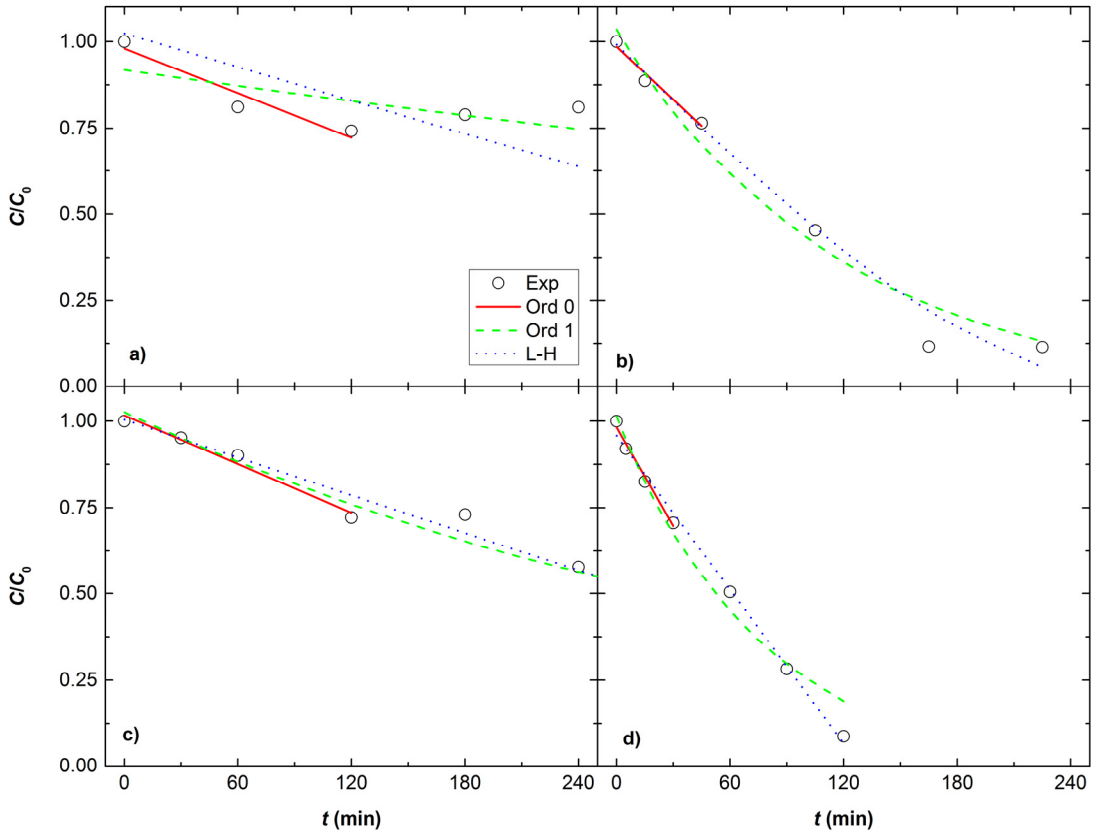

Figure S11. Pollutant degradation as a function of time using the N-TiO_2 photocatalyst for formic acid and white light (a), formic acid and UVA radiation (b), salicylic acid and white light (c), salicylic acid and UVA radiation (d). Data fits are including in the figures, using the pseudo-order zero (Ord 0), pseudo-order 1 (Ord 1), and Langmuir-Hinshelwood (L-H) models.

Relationship between the LVRPA, the quantum efficiency, and the kinetic models

Replacing the final expression of equation 1 in equation 4 (see Sect. 2.3 in the article), it is possible to see that

$$\eta_{rxn} = \frac{\langle v_0 \rangle_{V_R} V_R}{\langle \Phi_e \rangle_{A_w} A_w \eta_{abs}} \tag{S18}$$

where $\langle e^a \rangle_{V_R} = \eta_{abs} \langle \Phi_e \rangle_{A_w} A_w / V_R$ is the LVRPA averaged over the reactor volume (in Einstein·cm^{-3}·s^{-1}, where 1 Einstein = 1 mol of photons) [14]. Therefore, v_0 can be expressed as

$$v_0 = -\left.\frac{dC}{dt}\right|_0 = \eta_{rxn} \langle e^a \rangle_{V_R} \tag{S19}$$

where C is the concentration of the pollutant (in mol·cm^{-3}). This means that the initial rate of degradation is the product of a factor that depends on an intrinsic feature of the photocatalyst (the quantum efficiency) times a factor that depends on the reactor characteristics (the averaged LVRPA, equivalent to the total absorbed energy).

Taking into account equation S19, the following relationships exist between the parameters of each kinetic model, the LVRPA, and the quantum efficiency:

Order zero $$-\left.\frac{dC}{dt}\right|_0 = \eta_{rxn} \langle e^a \rangle_{V_R} = k_0 \tag{S20}$$

Order one $$-\left.\frac{dC}{dt}\right|_0 = \eta_{rxn} \langle e^a \rangle_{V_R} = kC_0 \tag{S21}$$

Langmuir-Hinshelwood $$-\left.\frac{dC}{dt}\right|_0 = \eta_{rxn} \langle e^a \rangle_{V_R} = \frac{k'KC_0}{1 + KC_0} \tag{S22}$$

References

1. Moreira J., Serrano B., Ortiz A., de Lasa H. (2010). Evaluation of Photon Absorption in an Aqueous TiO2 Slurry Reactor Using Monte Carlo Simulations and Macroscopic Balance, Ind. Eng. Chem. Res. 49, 10524–10534. https://doi.org/10.1021/ie100374f.
2. Siegel R., Howell J.R. Thermal radiation heat transfer, 4th ed, Taylor & Francis, New York, 2002.
3. Yokota T., Cesur S., Suzuki H., Baba H., Takahata Y. (1999). Anisotropic Scattering Model for Estimation of Light Absorption Rates in Photoreactor with Heterogeneous Medium, J. Chem. Eng. Jpn. 32, 314–321. https://doi.org/10.1252/jcej.32.314.